IRIS AperTO

UNIVERSITÀ DEGLI STUDI DI TORINO

AperTO - Archivio Istituzionale Open Access dell'Università di Torino

Fasudil treatment in adult reverses behavioural changes and brain ventricular enlargement in Oligophrenin-1 mouse model of intellectual disability

This is the author's manuscript

Original Citation:

Availability:

This version is available http://hdl.handle.net/2318/1620873 since 2016-12-21T14:36:59Z

Published version:

DOI:10.1093/hmg/ddw102

Terms of use:

Open Access

Anyone can freely access the full text of works made available as "Open Access". Works made available under a Creative Commons license can be used according to the terms and conditions of said license. Use of all other works requires consent of the right holder (author or publisher) if not exempted from copyright protection by the applicable law.

(Article begins on next page)

25 April 2024

HMG Advance Access published May 4, 2016

Title

Fasudil treatment in adult reverses behavioural changes and brain ventricular enlargement in Oligophrenin-1 mouse model of intellectual disability.

Author names and order

Hamid Meziane[3], Malik Khelfaoui[1,2*], Noemi Morello[4], Bassem Hiba[5], Eleonora Calcagno[4], Sophie Reibel-Foisset[6], Mohammed Selloum[3] ,Jamel Chelly[1,3], Yann Humeau,[2] Fabrice Riet[3], Ginevra Zanni[7], Yann Herault[3], Thierry Bienvenu[1], Maurizio Giustetto[4], Pierre Billuart[1].*

Affiliations:

1. Institut Cochin, INSERM U1016, CNRS UMR8104, Paris Descartes University, Paris, 75014, France.

malik.khelfaoui@gmail.com jamel.chelly@igbmcptsd.fr

thierry.bienvenu@inserm.fr pierre.billuart@inserm.fr

2. Institut interdisciplinaire de neuroscience, CNRS UMR5297, University of Bordeaux, Bordeaux, 33077, France.

yann.humeau@u-bordeaux.fr

3. PHENOMIN, Institut Clinique de la Souris, ICS; GIE CERBM, Institut de Génétique et de Biologie Moléculaire et Cellulaire, CNRS, UMR7104, INSERM, U964, University of Strasbourg, F-67404 Illkirch-Graffenstaden, France

meziane@igbmc.fr selloum@igbmc.fr

fabrice.riet@igbmc.fr herault@igbmc.fr

4. University of Torino, Department of Neuroscience « Rita Levi Montalcini », National Institute of Neuroscience-Italy, Torino, 10126, ITALY.

maurizio.giustetto@unito.it *eleonora.calcagno@unito.it*

noemi.morello@unito.it

5. Centre de Résonance Magnétique des Systèmes Biologiques, UMR 5536 CNRS, Université de Bordeaux, 33077, BORDEAUX.

bassem.hiba@u-bordeaux.fr

6. Chronobioton, CNRS, Universite Strasbourg, UMS3415, Strasbourg, 67084 France.

sreibel@neuro-cnrs.unistra.fr

7. Laboratory of Molecular Medicine, Unit of Neuromuscular and Neurodegenerative Disorders, Department of Neurosciences, Bambino Gesù Children's Hospital, IRCCS, 00165, Rome, Italy.

ginevra.zanni@opbg.net

: Co-1st authors

Corresponding author

Pierre BILLUART: Institut Cochin, 24 rue du Fg St Jacques, 75014, Paris, France pierre.billuart@inserm.fr, tel: 33 1 4441 2486, fax 33 1 4441 2421

© The Author 2016. Published by Oxford University Press. All rights reserved. For Permissions, please email: journals.permissions@oup.com

Downloaded from http://hmg.oxfordjournals.org/ by guest on May 5, 2016

Abstract

Loss of function mutations in human *Oligophrenin1 (OPHN1)* gene are responsible for syndromic intellectual disability (ID) associated with cerebellar hypoplasia and cerebral ventricles enlargement. Functional studies in rodent models suggest that *OPHN1* linked ID is a consequence of abnormal synaptic transmission and shares common pathophysiological mechanisms with other cognitive disorders. Variants of this gene have been also identified in autism spectrum disorder and schizophrenia. The advanced understanding of the mechanisms underlying Oligophrenin1-related ID, allowed us to develop a therapeutic approach targeting the RHOA/ROCK signalling pathway and repurpose Fasudil- a well-tolerated ROCK and PKA inhibitor- as a treatment of ID. We have previously shown *ex-vivo* its beneficial effect on synaptic transmission and plasticity in a mouse model of the OPHN1 loss of function.

Here, we report that chronic treatment in adult mouse with Fasudil, is able to counteract vertical and horizontal hyperactivities, restores recognition memory and limits the brain ventricular dilatation observed in *Ophn1*$^{-/y}$. However, deficits in working and spatial memories are partially or not rescued by the treatment. These results highlight the potential of Fasudil treatment in synaptopathies and also the need for multiple therapeutic approaches especially in adult where brain plasticity is reduced.

Downloaded from http://hmg.oxfordjournals.org/ by guest on May 5, 2016

Introduction

Intellectual Disability (ID) is defined by an overall Intelligence Quotient (IQ) lower than 70 associated with deficit in conceptual, social, and practical adaptive skills with an onset before the age of 18 years (1). The clinical spectrum of cognitive deficit varies widely from non-syndromic ID to Autism Spectrum Disorder (ASD) and is estimated to affect 3-5% of the population (2). The causes of ID are heterogeneous and include genetic and/or environmental factors that influence the development and function of the Central Nervous System (CNS) during the pre-, peri-, or post-natal period. Genetic causes are responsible for 40 to 50% of moderate to severe ID (IQ < 50), whereas environmental factors primarily contribute to mild ID (50 < IQ < 70) (1). Genes that are involved in ID with a preserved CNS organization (i.e., normal MRI scan) are likely to encode proteins that are necessary for the development of cognitive functions. Compelling evidence indicates that one major functional group of ID-related proteins corresponds to proteins that are enriched at synaptic compartments, and regulates synaptic activity (3, 4). Amongst them, several signalling molecules of the RhoGTPases pathway have been found mutated in ID patients (5).

Mutations in Oligophrenin1 gene (*OPHN1*), which encodes a RhoGAP are responsible for syndromic ID with moderate to severe cognitive impairment associated with cerebellar hypoplasia predominant in the vermis and brain ventricular enlargement (6-8). *Ophn1* gene loss of function in mouse mimics the human pathology apart the cerebellar hypoplasia (9). Compelling results from our group and others suggest that part of the ID in *OPHN1* patients is a consequence of abnormal synaptic transmission linked to enhanced RhoA signalling and deregulation of actin cytoskeleton at the inhibitory and excitatory synapse (10, 11). OPHN1 regulates clathrin-mediated endocytosis and the loss of its function reduces the internalization and recycling of synaptic vesicles and α-amino-3-hydroxy-5-methyl-4-isoxazolepropionic acid receptors (AMPAR) resulting in deficit in synaptic plasticity (12, 13). Disruption of OPHN1 and Homer1b/c protein interaction also results in the displacement of the endocytic zone from the Post-Synaptic Density (PSD) and impairs the addressing and recycling AMPAR (13). In addition *Ophn1* mRNA translation at the synapse is locally increased upon type1-metabolotropic receptors (mGluR1) activation suggesting that OPHN1 is a “mediator” of Long Term Depression (LTD) that controls the strength of the synapse during intense glutamatergic stimulation (14, 15). These functional deficits are associated with changes in the density and morphology of dendritic spines, the support of most excitatory synapses (9-11, 16). OPHN1 also interacts with Rev-erb alpha, a nuclear receptor that represses transcriptional activity of circadian clock genes delineating a new communication between synapse and nucleus (17). Because of hyperactivation of RHOA signalling pathway in *Ophn1* KO cells inhibiting one of its effector the RHO-kinases ROCK was able to restore synaptic transmission and plasticity in *Ophn1*$^{-/y}$ hippocampal slices (10, 12). More recently we discovered that not only ROCK but also Protein Kinase A (PKA) activities were increased in some brain regions of the *Ophn1*$^{-/y}$ mice (12). In this context, oral administration of Fasudil, a ROCK and PKA kinases inhibitor was able to rescue the fear extinction deficit observed in *Ophn1* KO mice (18)

In the present study, we expand these findings by targeting in vivo these pathways in adult mice and perform some neurological and behavioural phenotypic analysis focusing particularly on previously characterized deficits (9). Fasudil or HA1077, which is already used in Japan to cure cerebrovascular diseases was administered orally in adult during 3 months

Downloaded from http://hmg.oxfordjournals.org/ by guest on May 5, 2016

(19). It is a well-tolerated and safe molecule that crosses the brain blood barrier and its administration in rat models of Alzheimer improved their learning and memory performances (20). Altogether, this result encourages preclinical trials for additional indications in neurodevelopmental diseases such as the OPHN1 linked ID.

Results

Inhibition of the RHOA/RHO-kinase and PKA signalling pathways in *Ophn1*$^{-/y}$ mouse brain

As a GAP protein, OPHN1 stimulates GTPase activity of RHOA and lowers the effector activity of the Rho kinase, ROCK (figure 1A). We previously showed that RHOA/ROCK pathway is over-activated in *Ophn1*$^{-/y}$ leading to the increase of ROCK's target phosphorylation such as the myosin phosphatase target subunit-1 (MYPT1) *(12)*. MYPT1 phosphorylation by ROCK reduces the phosphatase activity toward the Myosin light chain (MLC) resulting in the increase of acto-myosin contraction *(21)*. Ex vivo treatments by the ROCK inhibitors Y27632 or Fasudil decreased the phosphorylation of MYPT1, restored the endocytosis deficit in astroglial cells, the inhibitory and excitatory transmissions, the synaptic plasticity and network activity in hippocampal slices from the KO mice *(10, 12, 22)*. We more recently identified higher PKA activities in the cortex and hippocampus of *Ophn1*$^{-/y}$ resulting in a deficit of Long-Term Potentiation (LTP) at cortico-Lateral Amydala synapses together with a deficit in fear extinction memory *(18)*. Daily administration of Fasudil at 3 mg during 3 weeks by oral administration was able to restore the level of PKA activity to controls and also the behaviour of the *Ophn1*$^{-/y}$ with little effect on *Ophn1*$^{+/y}$ *(18)*. Whereas the molecular links between these two pathways in the context of loss of OPHN1 function are still unclear, the dosage and the route of administration of Fasudil encourage to the therapeutic schemas that we used in this new study: adult males of 2 or 4 months were given orally a daily dose of 3 mg for a total of 3 months (figure 1B and 1C). Behaviour, brain anatomy (RMI) and dendritic spine morphology were evaluated during and after the 3 months of treatment.

Fasudil restores body weight, hyperactivity, and motor ability phenotypes in *Ophn1*$^{-/y}$ mice

We previously reported that loss of OPHN1 function in mice leads to novelty-driven hyperactivity, decreases lateralization and alters spatial memory with no or little effect on motor coordination, on anxiety related behaviours and in social interactions (9). Therefore we tested whether ROCK/PKA inhibitions alters some behavioural parameters in *Ophn1*$^{+/y}$ and could rescue some of the phenotypes observed in *Ophn1*$^{-/y}$. Chronic Fasudil treatment did not affect the survival rate of animals and we did not notice any side effects of Fasudil on the general behaviour of the treated animals. No effects on body weight or on motor coordination were observed after Fasudil treatment of *Ophn1*$^{+/y}$ (data not shown). *Ophn1*$^{-/y}$ males showed significantly decreased body weight, as compared to *Ophn1*$^{+y}$ (29.23+/-0.93 vs 31.65+/-0.70; genotype $F_{(1,38)}$=4.58; $p<0.05$, *post-hoc* test $p<0.05$), such effect was corrected by Fasudil treatment (data not shown) and also tend to have reduced motor coordination in the rotarod task (figure 2A). In the elevated plus maze, the percentage of entries and the percentage of time in the open arms were comparable between genotypes and between treatments,

Downloaded from http://hmg.oxfordjournals.org/ by guest on May 5, 2016

suggesting that neither *Ophn1* deletion nor Fasudil treatment affected anxiety in this test (data not shown).

We next explored the hyperactivity phenotype in different situations. In the elevated plus maze (Figure 2B) and also during the first 5 minutes of habituation phase of the object recognition task (Figure 2C), *Ophn1*$^{-/y}$ males showed significantly increased number of rears as compared to *Ophn1*$^{+/y}$, a phenotype that was rescued by Fasudil without any effect on *Ophn1*$^{+/y}$ (Figure2B: interaction genotype x treatment $F_{(1,36)}$=7.32; *p<0.05*, *post-hoc* test *Ophn1*$^{+/y}$ (control) vs *Ophn1*$^{-/y}$ (control) *p<0.05*, *post-hoc* test *Ophn1*$^{-/y}$ (control) vs *Ophn1*$^{-/y}$ (Fasudil) *p<0.05* and Figure 2C : interaction genotype x treatment $F_{(1,37)}$=7.19, *p<0.05*; treatment $F_{(1,37)}$=4.75, *p<0.05*; *post-hoc* test *Ophn1*$^{+/y}$ (control) vs *Ophn1*$^{-/y}$ (control) *p<0.05*, *post-hoc* test *Ophn1*$^{-/y}$ (control) vs *Ophn1*$^{-/y}$ (Fasudil) *p<0.01*). The observed hyperactivity in *Ophn1*$^{-/y}$ not only affects the rearing but also the locomotor activity. During the first 5 minutes of the habituation phase in the object recognition task *Ophn1*$^{-/y}$ mice travelled a longer distance in the open field compared to *Ophn1*$^{+/y}$ (Figure2D) (genotype $F_{(1,38)}$=4.10, *p<0.05*; *post-hoc* test *Ophn1*$^{+/y}$ (control) vs *Ophn1*$^{-/y}$ (control) *p<0.05*). Fasudil treatment restores the locomotor activity back to untreated control genotype (Figure 2D) (treatment $F_{(1,38)}$=4.83, *p<0.05*; *post-hoc* test *Ophn1*$^{-/y}$ (control) vs *Ophn1*$^{-/y}$ (Fasudil) *p<0.05*). In addition, both locomotors and rearing activities were also increased in *Ophn1*$^{-/y}$ mice during the acquisition trial of object recognition (supplemental figure 1). In this context Fasudil also restored similar levels to *Ophn1*$^{+/y}$ mice. Altogether Fasudil chronic treatment largely improves the *Ophn1*$^{-/y}$ condition regarding the hyperactivity.

Improvement of recognition but not working and spatial reference memory deficits

In the recognition task animals were allowed to discriminate between a novel object and a familiar one. Neither genotype nor treatment alters significantly the object recognition performance (Figure 3A) (overall statistical analysis with 2 way ANOVA). Nevertheless, vehicle-treated *Ophn1*$^{+/y}$, Fasudil-treated *Ophn1*$^{+/y}$ and Fasudil-treated *Ophn1*$^{-/y}$, but not vehicle-treated *Ophn1*$^{-/y}$, showed recognition performance significantly above the 50% chance level (*p<0.05*), which might suggest altered recognition memory in mutants, and protective effect of Fasudil (Figure 3A).
In the previous characterization of the *Ophn1*$^{-/y}$ (9), we reported the hyperactivity of the mice in the Y-maze task but did not explore the spontaneous alternation as a measure of the working memory. We now extended these first studies and found that loss of OPHN1 function reduces the frequency of spontaneous alternation (genotype $F_{(1,38)}$=2.84, *p<0.10*; *post hoc* test *Ophn1*$^{+/y}$ (control) vs *Ophn1*$^{-/y}$ (control) *p<0.05*). Even if not striking, such deficits were reduced in ophn1$^{-/y}$ treated with Fasudil; their performance was statistically comparable to that of *Ophn1*$^{+/y}$ groups. This observation suggests, even with reduced strength, that Fasudil has potency to rescue working memory deficits, supporting data observed in the object recognition task (Figure 3B).

Next we investigated the effect of Fasudil on the spatial reference memory phenotype linked to *Ophn1* deficiency. The latency (data not shown) and distance (Figure 3C) to locate a submerged platform decreased significantly in all groups of mice as testing progressed (*Ophn1*$^{+/y:}$ learning $F_{(4,100)}$=28.55, $p<10^{-4}$ and *Ophn1*$^{-/y}$: learning $F_{(4,90)}$=14.23, $p<10^{-4}$). On the other hand, a significant effect of genotype was observed concerning these parameters (vehicle: genotype $F_{(1,95)}$=12.67, *p<0.001*, and Fasudil: genotype $F_{(1,95)}$=13.01, *p<0.001*). *Ophn1*$^{-/y}$ mice, whatever the treatment, showed significantly longer latencies (data not

Downloaded from http://hmg.oxfordjournals.org/ by guest on May 5, 2016

shown) and distances to the hidden platform, as compared to *Ophn1*$^{+/y}$ counterparts (Vehicle: *post hoc* tests $p<0.05$ for days 2 and 3 and Fasudil: *post hoc* tests $p<0.01$ for day 3), confirming the delayed spatial learning in *Ophn1*$^{-/y}$ (9) and showing little or no improvement after treatment. In agreement with this observation, the preference for the target quadrant (data not shown) and the number of platform crosses (Figure 3D) were reduced in *Ophn1*$^{-/y}$ mice (genotype $F_{(1,38)}=13.02$, $p<0.001$, vehicle *post-hoc* test $p<0.05$) with no effect of Fasudil.

Reduction of the brain ventricle dilatation

To investigate Fasudil effect on brain anatomy, 6 fixed brains from each group of animals were processed for magnetic resonance imaging (MRI). Two *Ophn1*$^{-/y}$ males from the untreated group displayed hydrocephalus and were excluded from the analysis. First, we measured the whole brain volume and did not notice any effect of the genotype or the treatment on this parameter (Figure 4C-D). In accordance with our previous study (9), untreated *Ophn1*$^{-/y}$ mice show an increase of the relative ventricular size compared to their *Ophn1*$^{+/y}$ counterparts (genotype $F_{(1,18)}=7.00$, $p<0.05$; untreated *Ophn1*$^{-/y}$ *vs* *Ophn1*$^{+/y}$ *post hoc* test $p<0.05$) (Figure 4A-B). Fasudil treatment tends to decrease the size of the ventricle of *Ophn1*$^{-/y}$ with no effect on *Ophn1*$^{+/y}$ ($F_{(1,18)}=4.99$, $p<0.05$; untreated *vs* treated *Ophn1*$^{-/y}$ *post hoc* test $p< 0,10$) (Figure 4A-B). In conclusion, inhibition of RHO kinase ameliorates the brain lateral ventricular dilatation observed in *Ophn1* deficient mice and limits the development to hydrocephaly. Indeed none of the six treated *Ophn1*$^{-/y}$ mice were affected by this condition.

Genotype-specific response of dendritic spine morphology

Ophn1 deletion reduced the density of mushroom-shaped dendritic spines decorating apical dendrites in CA1 region of hippocampus in 8-week-old mice (8). In this study we used a Diolistic approach to fluorescently label dendrites and spines of pyramidal neurons in the same hippocampal area (23). In order to explore the effect of ROCK inhibition, we treated 8-week-old *Ophn1*$^{+/y}$ and *Ophn1*$^{-/y}$ male mice with Fasudil or vehicle solution for 12 weeks (figure 1C). Five-month-old mice of the four experimental groups (n = 2/4 animals/group) were processed for morphological analyses of dendritic spines on and apical dendrites imaged 100-200 µm away from the soma (figure 5A).
We found that while dendrites from *Ophn1*$^{+/y}$ and *Ophn1*$^{-/y}$ mice were decorated with similar density of mushroom-, thin-shaped (figure 5C and D) and stubby spines (data not shown), the density of filopodia protrusions was significantly increased in *Ophn1*$^{-/y}$ mice (figure 5B). Also, no significant differences of spine morphology (i.e. head diameter and neck length) were observed between genotypes (figure 5 E,F and data not shown). However, we observed that Fasudil treatment produced genotype-specific effects on both the density and the morphology of dendritic spines. Interestingly, Fasudil specifically increased the density of thin-shaped spines in *Ophn1*$^{+/y}$ mice when compared to untreated animals (figure 5C; $p < 0.05$). Moreover our analyses revealed that after Fasudil treatment, *Ophn1*$^{-/y}$ mice presented with an higher number of mushroom-shaped spines and a lower number of thin-shaped spines than treated *Ophn1*$^{+/y}$ animals (figure 5D and 5C; Two-way ANOVA. mushroom: (interaction), $F_{(1,10)} = 5.34$, $p = 0.043$; (genotype), $F_{(1,10)} = 7.96$, $p = 0.018$; (Fasudil) $F_{(1,10)} = 1.57$, $p = 0.238$. thin: (interaction), $F_{(1,10)} = 9.96$, $p = 0.010$; (genotype), $F_{(1,10)} = 9.13$, $p = 0.013$; (Fasudil) $F_{(1,10)} = 7.05$, $p= 0.024$). In addition, Fasudil treatment produced no effects on the density stubby spines (data not shown). Intriguingly, Fasudil treatment was able to rescue the abnormal number of filopodia shown by *Ophn1*$^{-/y}$ mice (figure 5B; Two-way ANOVA. filopodia: (interaction), $F_{(1,10)} = 1.28$, $p = 0.285$; (genotype), $F_{(1,10)} = 4.95$, $p = 0.049$;

Downloaded from http://hmg.oxfordjournals.org/ by guest on May 5, 2016

(Fasudil) $F_{(1,10)}$ = 2.21, p = 0.168). Moreover, we found that after Fasudil treatment *Ophn1*$^{-/y}$ mice showed shorter neck-length of mushroom-shaped spines and smaller head-diameter of thin-shaped spines than treated *Ophn1*$^{+/y}$ animals (figure 5E and 5F; Two-way ANOVA. mushroom neck lenght: (interaction), $F_{(1,10)}$ = 6.04, p = 0.034; (genotype), $F_{(1,10)}$ = 8.17, p = 0.017; (Fasudil) $F_{(1,10)}$ = 0.73, p = 0.412. thin head diameter: (interaction), $F_{(1,10)}$ = 1.33, p = 0.276; (genotype), $F_{(1,10)}$ = 10.21, p = 0.010; (Fasudil) $F_{(1,10)}$ = 1.62, p= 0.232). Altogether, we found that compared to untreated *Ophn1*$^{+/y}$ animals dendritic spines are normalized in *Ophn1*$^{-/y}$ mice after 5 months of age while the density of filopodia protrusion is increased, and that Fasudil treatment differentially affects the dendritic spines in *Ophn1*$^{+/y}$ and *Ophn1*$^{-/y}$ mice.

Discussion

The advanced understanding of pathophysiological mechanisms underlying *OPHN1*-related ID, allowed us to develop a therapeutic approach targeting the RHOA/ROCK and PKA pathways and reposition a pharmacological drug Fasudil for ID treatment. Previous in vitro and ex-vivo experiments have demonstrated the beneficial effect of ROCK and PKA inhibitions on synaptic transmission and on fear conditioning (10, 12, 18, 22).

Here we test in the *Ophn1*$^{-/y}$ mouse whether Fasudil administration rescues other behavioural deficits and brain anatomy alterations. This study allowed us to replicate the differences between genotype on an independent cohort raised in a different location. Finally we shows that chronic treatment of adult male for 3 months counteracts the brain ventricular dilatation (BVD) and also novelty driven hyperactivity but has little beneficial effects on spatial working and reference memories.

Part of the ID in *OPHN1* patients is a consequence of a synaptopathy with abnormal synaptic transmission linked to enhanced RHOA and PKA signalling and deregulation of actin cytoskeleton at the inhibitory and excitatory synapses. These functional deficits are associated with changes in neuronal morphology mainly affecting the dendritic spines, which support most of the excitatory synapses (9-11, 16). Acute treatment by the specific ROCK inhibitor Y27632 in hippocampus restores excitatory and inhibitory transmissions without rescuing the dendritic spines phenotypes suggesting that either alterations of spine is a consequence of transmission deficit or that the morphological response is delayed compared to the synaptic transmission (10). Here, we found that the dendritic spine density and morphology of CA1 pyramidal neurons from *Ophn1*$^{-/y}$ are similar to controls at 5 months old (this study) while *Ophn1*$^{-/y}$ retained an higher density of dendritic filopodia, an immature type of dendritic protrusion which density was found abnormally elevated in both autism (24) and Fragile-X (25) conditions. When compared to other studies in hippocampus at different ages (9, 10) (supplemental figure 2A) the differences between genotype seems to attenuate suggesting some compensation of dendritic spine density with age similarly to what was observed in the Rett mouse model (23). Interestingly we recently showed that PKA activity is increased in some brain regions including the hippocampus but the link between *Ophn1* deficit and this increase is still unknown (18). RHOA phosphorylation by PKA is known to reduce RHOA activation by decreasing ROCK binding to phosphorylated RHOA (26). Therefore the increase of PKA would compensate for the deficit in *Ophn1* and would restore the balance between RHO and RAC GTPases, which are known to have opposite effect on dendritic spine growth (supplemental figure 2B and 2C). More surprisingly, we found that the two genotypes show a differential response to RHO kinase inhibition by Fasudil regarding the density and morphology of either mature (i.e. mushroom) or immature (i.e. thin) type of

Downloaded from http://hmg.oxfordjournals.org/ by guest on May 5, 2016

spines. Whereas Fasudil increases the density of thin spines in *Ophn1*$^{+/y}$, it has no effect in *Ophn1*$^{-/y}$. In contrast, after Fasudil treatment *Ophn1*$^{-/y}$ show higher mushroom spines density than *Ophn1*$^{+/y}$. Morever, while Fasudil produces a decrease in the head size of thin spines only in *Ophn1*$^{-/y}$, it resulted in longer neck length of mushroom spines only in *Ophn1*$^{+/y}$. These differential effects of the treatments between genotype may reflect the different functions of ROCK1 and ROCK2 in the dendritic spines and the different role of OPHN1 in the control of their kinase activity (27). Alternatively, compared to the specific ROCK inhibitor Y27632, Fasudil also inhibits PKA activity with a similar efficacy (18, 28). The differential effects of Fasudil on neck length would be the consequence of the triple inhibition of the pathway in *Ophn1*$^{+/y}$ whereas, in *Ophn1*$^{-/y}$, persistent activated RHOA will stimulate alternative effectors pathway such as CITRON/CORTACTIN/COFILIN/F-ACTIN to induce the dendritic spine retraction (29) (supplemental figure 2B and 2C). Interestingly, RHOA phosphorylation by PKA alters specifically ROCK binding but not other effectors to the GTPase (26).

Human mutations in *OPHN1* gene lead to ID together with cerebellar hypoplasia and BVD (7, 8). Whereas the cerebellar phenotype is not reproduced in the mouse model, we previously showed that BVD is already present in *Ophn1*-/y mice at weaning (22%) and worsen with age (70% at 8-9 months)(9). The pathophysiological mechanism of the BVD is still not known but several hypotheses could be made. *OPHN1* is highly expressed in the vascular endothelium (16, 30) and the loss of its function would alter vascular permeability due to activation of RHOA/ROCK pathway in these cells (31). Brain exposure to blood is detrimental and can lead to hydrocephaly when it occurs during foetal period and also to ventriculomegaly in postnatal brain (32). Pharmacological inhibition of ROCK has been to shown to decrease vascular permeability (33) and, in the context of *Ophn1*$^{-/y}$, Fasudil would limit the exposure of the brain to blood. Alternatively *OPHN1* is expressed in the choroid plexuses and in the ependyma lining the brain ventricles (data not shown), which are two structures involved in the production and circulation of the cerebro spinal fluid (CSF). *OPHN1* through the regulation of actin cytoskeleton may affect cilia morphology and/or function. However we observed no defect of cilia morphology in *Ophn1*$^{-/y}$ by transmission electronic microscopy (data not shown). Further investigations are required to explore the pathophysiological mechanisms of BVD and its rescue by Fasudil.

Several animal models with hippocampal lesions (34) or with mutations affecting glutamate transmission (35, 36) show increased locomotor activity in various test, which has been commonly associated to an excess of exploratory activity when exposed to a novel environment. *Ophn1*$^{-/y}$ mice, which have some alterations in excitatory and inhibitory transmissions in hippocampus (10, 12, 22) and in other brain locations (18) display a hyperactivity phenotype mainly during the first 10 minutes after its introduction into another context. The increase of both vertical (rearing) and horizontal (locomotor) movements could reflect an excess of curiosity or an uncontrolled response to the stress. Interestingly, *Ophn1*$^{-/y}$ mice hyperactivity is completely abolished by Fasudil administration without detrimental effect in *Ophn1*$^{+/y}$.

Although chronic administration of Fasudil in adult improved recognition memory and rescued extinction memory deficits in *Ophn1*$^{-/y}$, it had no effect on spatial reference memory deficit (Morris Water Maze) (this study and (18)). In some tests (Figure 3B and 3D) Fasudil treatment even tends to have detrimental effects on *Ophn1*$^{+/y}$ resulting on an apparent rescue due to loss of significant differences between treated mice of both genotypes (Y maze). Previous studies in hippocampal slice have shown that synaptic transmission and

Downloaded from http://hmg.oxfordjournals.org/ by guest on May 5, 2016

plasticity but also network activities are rescued by acute ROCK inhibition using Y27632 (10, 12, 22). In some of these studies the rescue efficacy depends on the tested conditions. Whereas spontaneous gamma oscillations in CA3 region of *Ophn1*$^{-/y}$ hippocampus are restored back to control level, kainate-induced oscillations are not (22). Similarly, Fasudil administration rescued cued fear conditioning extinction but not contextual conditioning memories (18). In the present study, the reduced beneficial effect *in vivo* on memory tests suggest that some neurodevelopmental alterations during the embryo and perinatal periods may not be compensated later by treatment at the adult stage. This hypothesis will deserve a new study starting the Fasudil treatment earlier during middle gestation (E15 days post-coïtum) in order to restore the balance in RHO GTPase and PKA activation during the pic of neurogenesis (37). An alternative strategy to treat adult would be to reactivate the juvenile plasticity and reopen the developmental window in the adult brain using antidepressant drugs such as fluoxetine (38, 39) and then perform intensive training together with the administration of Fasudil. This strategy would restore the synaptic transmission and plasticity in a permissive context to rebuild new “improved” activity networks during the acquisition and consolidation of deficient cognitive functions.

Downloaded from http://hmg.oxfordjournals.org/ by guest on May 5, 2016

Materials and Methods

Animals and Fasudil treatment

Two cohorts of male mice in C57BL/6N genetic background were randomly divided into four groups and experiments were conducted blindly to the animal caretakers and investigators. Fasudil hydrochloride or HA1077 (F4660, LC laboratories, Boston, MA, USA) was given orally ad libitum in drinking water (100 mg/kg/day). Drinking volumes (4.6ml/day) were similar between treated and untreated mice.

Four weeks after the start of Fasudil delivery, 17-18 weeks-old mice from the first cohort (10-12 per genotype and per treatment) underwent behavioural tests that lasted 8 weeks during which they were kept under treatment. At the end of this study, half of the animals from each group (genotype and treatment) were perfused with 4% paraformaldehyde for MRI analysis. For the other half of mice, brain regions were sampled, snap frozen, then maintained at -80°C for subsequent molecular analysis. Animals displaying hydrocephaly were excluded from subsequent analyzes.

Another cohort of mice (8 week-old) was treated for 12 weeks before dendritic spine were analysed.

Testing was carried out in accordance with the EC directive 2010/63/UE and application decree 2013-118 dated 1st February 2013 and with the agreement of the local ethical committee Com'Eth (n°17) under the accreditation numbers 2012-019 and 2012-139 with YH as the principal investigator (accreditation 67-369).

Behaviour

The general health and basic sensory motor functions were evaluated using a modified SHIRPA protocol (40). It provides an overview of physical appearance, body weight, body temperature, neurological reflexes and sensory abilities. Detailed procedures for evaluation of motor function (rotarod test), anxiety-related behaviour (elevated plus maze, openfield) and learning and memory (object recognition task, Y maze and Morris water maze) were previously described (41) and briefly summarize below.

Elevated plus maze: The apparatus used was completely automated and made of PVC (Imetronic, Pessac, France). It consisted of two open arms (30 X 5 cm) opposite one to the other and crossed by two enclosed arms (30 X 5 X 15 cm). The apparatus was equipped with infrared captors allowing the detection of the mouse in the enclosed arms and different areas of the open arms. The number of entries into and time spent in the open arms were used as an index of anxiety. Closed arm entries were used as measures of general motor activity. The number of rears in the closed arms, as well as ethological parameters such as stretching, attempts and head dips, was also automatically scored.

Object recognition task: The object recognition task was performed in automated open fields. The open-fields were placed in a room homogeneously illuminated at 70 Lux at the level of each open field. The objects to be discriminated were a glass marble (2,5 cm diameter) and a plastic dice (2 cm). Animals were first habituated to the open-field for 30 min. The next day, they were submitted to a 10-minutes acquisition trial during which they were placed in the open-field in presence of an object A (marble or dice). The time the animal took to explore

Downloaded from http://hmg.oxfordjournals.org/ by guest on May 5, 2016

the object A (when the animal's snout was directed towards the object at a distance ≤ 1 cm) is manually recorded. A 10-minutes retention trial is performed 3 h later. During this trial, the object A and another object B are placed in the open-field, and the times tA and tB the animal takes to explore the two objects are recorded. A recognition index (RI) is defined as (tB / (tA + tB)) x100.

Y-maze spontaneous alternation: The apparatus was a Y-maze made of Plexiglas and having 3 identical arms (40x9x16 cm) placed at 120° from each others. Each arm had walls with specific motifs allowing distinguish it from the others. Each mouse was placed at the end of one of the three arms, and allowed to explore freely the apparatus for 5min, with the experimenter out of the animal's sight. Alternations are operationally defined as successive entries into each of the three arms as on overlapping triplet sets (i.e., ABC, BCA ...). The percentage of spontaneous alternation was calculated as index of working memory performance. Total arm entries and the latency to exit the starting arm were also scored as indexes of ambulatory activity and emotionality in the Y- maze, respectively.

Morris water maze: The water maze consisted of a white circular tank (1.50 m diameter) filled with opaque water. Pool temperature was adjusted to 21+1°C. For the hidden platform task, the escape platform (10 cm diameter) was positioned 1cm below water level in the centre of one of the pool quadrants. For the cued task, platform position was signaled by the addition of a small flag. The walls surrounding the water maze were hung with posters and flags, which served as visual cues and were visible during all stages of training and testing. Movement of the mice within the pool was tracked and analyzed with a computerized tracking system (ViewPoint, France).

Animals were first trained in the hidden platform protocol (spatial learning). Mice were required to locate a submerged hidden platform by using only extra-maze cues. Each mouse received 5 blocks of training trials over five consecutive days in which they were placed in the pool at one of four randomized start positions, and allowed to locate the hidden platform. Trials lasted for a maximum of 120s and were separated by 15-20 min intervals. If a mouse failed to find the platform within this period, it is guided to its position by the experimenter. Spatial learning performance was assessed during a probe trial 1h after training, and for which the target platform was removed from the pool.

Mice were then tested for cued training (visible platform), in which they were placed in the pool facing the edge at one of four start positions (NE, SE, SW, NW), and required to locate a flagged platform whose position varied across trials. Each mouse received 4 trials per day for 2 consecutive days. Trials lasted for a maximum of 120s and were separated by 15-20 min intervals. If a mouse failed to find the platform within this period, it is guided to its position by the experimenter.

The latency, distance and the average speed were used to evaluate performance during training trial. For the probe trial, the percentage of time in each quadrant and the number of platform crosses were used as index of spatial learning performance.

Magnetic resonance imaging (MRI): acquisition and analysis

Fixed brains were included in agarose and imaged with a 9.4T nuclear magnetic resonance scanner (Bruker BioSpin, Ettlingen, Germany). Fast spin echo pulse sequence was used for

Downloaded from http://hmg.oxfordjournals.org/ by guest on May 5, 2016

T_2-weighted imaging with following parameters: TR = 4.7 s and effective TE = 22.4 ms, echo train length = 8 echos. Multiple slice 2D images were acquired with in-plane imaging matrix 192 x 168 and field of view 20 x 20 mm^2. Thickness of slices was 0.4 mm without gap between slices. Slice number was 60, covering the whole brain. The imaging resolution was 0.1 x 0.12 x 0.4 mm^3. A total of six mice per group were scanned. The images were processed using Amira (TGS, San Diego, CA, USA). The entire brain and the ventricles were manually delineated for each slice and their 3D volumes were measured.

Dendritic spine analysis

Dendritic spines labeling was performed as in (23). Briefly, DiI (1,1′-dioctadecyl-3,3,3′,3′-tetramethylindocarbocyanine perchlorate crystals, Invitrogen, USA) was dissolved in methylene chloride (Supelco), dropped onto the tungsten particles (1.3 mm in diameter; Bio-Rad). DiI-coated particles were injected in Tygon tubing subsequently cut into small pieces (bullets). Mice were anesthetized with an intraperitoneal injection of Avertin and perfused with PBS, and then with 4% PFA in 0.1 M PB. Brains were postfixed in the same solution, washed several times in PB 0.1 M, and then cut into 300 µm sections on a vibratome (Leica VT 1000S). An helios gene gun system (Bio-Rad) was used to propel DiI-coated particles into fixed slices. After the shot, the slices were placed in 4% PFA for 2 h, washed three times in PB 0.1 M, mounted on glass slides. Images from fluorescently labeled apical dendrites (100-200 µm from the soma) in the CA1 region of hippocampus were acquired using a LSM-5 Pascal confocal microscope (Zeiss, Göttingen, Germany) with HeNe (543 nm) laser. To generate the dataset, ≥10 *z*-stack images consisting of 10–15 sections (512 × 512 pixels, 80 to 100 µm-long dendritic segments) spaced 0.5 µm apart were collected for each animal. Dendritic segments and spines were analyzed with ImageJ software (NIH, public domain), with an observer blinded to the genotype and experimental conditions. Spine were classified as filopodia (protrusions without an enlargement of the tip), thin (protrusions with a head smaller than spine length), mushroom (large head spines with a neck) or stubby (large head spines without a neck). Only dendritic protrusions that were clearly projecting out of the shaft were measured. The following morphological parameters were calculated: density of specific spine classes, neck lenght (the linear distance from the junction with the dendritic shaft to that with the spine head) and head diameter (measured along the dimension that maximized head width). Density analysis were expressed as number of dendritic spine/µm.

Statistical analysis and graph representation.

Two-way analyzes of variance (ANOVA) followed by Bonferroni or Sidak's post hoc multiple comparison tests were used to analyze the contribution of the genotype and the treatment to the variability of each test. One sample t-test was also used to complete the analysis of the Recognition index and the dendritic spine phenotypes. Only significant results are detailed. We used GraphPad Prism (La Jolla, CA, USA) to perform statistical analyses and draw graphical representations.

In all figures, data are presented with histogram bars expressing the mean together with the standard error of the mean (sem). *: significant difference between genotypes (*Ophn1*$^{+/y}$ and

Downloaded from http://hmg.oxfordjournals.org/ by guest on May 5, 2016

Ophn1$^{-/y}$ mice); #: significant difference between treated (Fasudil) and untreated mice (Control=Vehicle); $: significant difference with theoretical value (p<0.05).

Funding:

This work *was* supported by the Fondation Jerome Lejeune to PB and by Compagnia di Sanpaolo (Italy) to GM. This study also received support from French state funds through the "Agence Nationale de la Recherche (ANR)" under the frame programs "Investissements d'Avenir" labelled "HR-DTI" ANR-10-LABX-57 funded by the TRAIL to HB and ANR-10-IDEX-0002-02, ANR-10-LABX-0030-INRT, ANR-10-INBS-07 PHENOMIN to YH as well as from the EU FP7 large-scale integrated project GENCODYS (FP7-COLLABORATION PROJECT-2009-2.1.1-1/241995) to YH, JC and PB.

Acknowledgments:

I would like to acknowledge Nathalie Spassky (ENS, Paris, France) and Jean-Marc Corsi (UVSQ, Versailles, France) for analyzes by TEM of brain ventricular walls.

Downloaded from http://hmg.oxfordjournals.org/ by guest on May 5, 2016

References:

1. van Bokhoven,H. (2011) Genetic and Epigenetic Networks in Intellectual Disabilities. **45**, 81–104.

2. Srivastava,A.K. and Schwartz,C.E. (2014) Intellectual disability and autism spectrum disorders: Causal genes and molecular mechanisms. *Neuroscience and Biobehavioral Reviews*, 10.1016/j.neubiorev.2014.02.015.

3. Boda,B., Dubos,A. and Muller,D. (2010) Signaling mechanisms regulating synapse formation and function in mental retardation. *Current Opinion in Neurobiology*, **20**, 519–527.

4. Pavlowsky,A., Chelly,J. and Billuart,P. (2011) Emerging major synaptic signaling pathways involved in intellectual disability. *Molecular Psychiatry*, **17**, 682–693.

5. Ba,W., van der Raadt,J. and Kasri,N.N. (2013) Rho GTPase signaling at the synapse_ Implications for intellectual disability. *Experimental Cell Research*, **319**, 2368–2374.

6. Billuart,P., Bienvenu,T., Ronce,N., Portes,des,V., Vinet,M.C., Zemni,R., Roest Crollius,H., Carrie,A., Fauchereau,F., Cherry,M., *et al.* (1998) Oligophrenin-1 encodes a rhoGAP protein involved in X-linked mental retardation. *Nature*, **392**, 923–926.

7. Chabrol,B., Girard,N., N'Guyen,K., Gérard,A., Carlier,M., Villard,L. and Philip,N. (2005) Delineation of the clinical phenotype associated withOPHN1 mutations based on the clinical and neuropsychological evaluation of three families. *Am. J. Med. Genet.*, **138A**, 314–317.

8. Zanni,G., Saillour,Y., Nagara,M., Billuart,P., Castelnau,L., Moraine,C., Faivre,L., Bertini,E., Durr,A., Guichet,A., *et al.* (2005) Oligophrenin 1 mutations frequently cause X-linked mental retardation with cerebellar hypoplasia. *Neurology*, **65**, 1364–1369.

9. Khelfaoui,M., Denis,C., van Galen,E., de Bock,F., Schmitt,A., Houbron,C., Morice,E., Giros,B., Ramakers,G., Fagni,L., *et al.* (2007) Loss of X-Linked Mental Retardation Gene Oligophrenin1 in Mice Impairs Spatial Memory and Leads to Ventricular Enlargement and Dendritic Spine Immaturity. *Journal of Neuroscience*, **27**, 9439–9450.

10. Powell,A.D., Gill,K.K., Saintot,P.-P., Jiruska,P., Chelly,J., Billuart,P. and Jefferys,J.G.R. (2012) Rapid reversal of impaired inhibitory and excitatory transmission but not spine dysgenesis in a mouse model of mental retardation. *The Journal of Physiology*, **590**, 763–776.

11. Nadif Kasri,N., Nakano-Kobayashi,A., Malinow,R., Li,B. and Van Aelst,L. (2009) The Rho-linked mental retardation protein oligophrenin-1 controls synapse maturation and plasticity by stabilizing AMPA receptors. *Genes & Development*, **23**, 1289–1302.

12. Khelfaoui,M., Pavlowsky,A., Powell,A.D., Valnegri,P., Cheong,K.W., Blandin,Y., Passafaro,M., Jefferys,J.G.R., Chelly,J. and Billuart,P. (2009) Inhibition of RhoA pathway rescues the endocytosis defects in Oligophrenin1 mouse model of mental retardation. *Human Molecular Genetics*, **18**, 2575–2583.

13. Nakano-Kobayashi,A., Kasri,N.N., Newey,S.E. and Van Aelst,L. (2009) The Rho-linked mental retardation protein OPHN1 controls synaptic vesicle endocytosis via endophilin A1. *Current biology : CB*, **19**, 1133–1139.

14. Nadif Kasri,N., Nakano-Kobayashi,A. and Van Aelst,L. (2011) Rapid Synthesis of the X-

Downloaded from http://hmg.oxfordjournals.org/ by guest on May 5, 2016

Linked Mental Retardation Protein OPHN1 Mediates mGluR-Dependent LTD through Interaction with the Endocytic Machinery. *NEURON*, **72**, 300–315.

15. Di Prisco,G.V., Huang,W., Buffington,S.A., Hsu,C.-C., Bonnen,P.E., Placzek,A.N., Sidrauski,C., cacute,K.S.I.K., Kaufman,R.J., Walter,P., *et al.* (2014) Translational control of mGluR-dependent long-term depression and object-place learning by eIF2&alpha. 10.1038/nn.3754.

16. Govek,E.E., Newey,S.E., Akerman,C.J., Cross,J.R., Van der Veken,L. and Van Aelst,L. (2004) The X-linked mental retardation protein oligophrenin-1 is required for dendritic spine morphogenesis. *Nat Neurosci*, **7**, 364–372.

17. Valnegri,P., Khelfaoui,M., Dorseuil,O., Bassani,S., Lagneaux,C., Gianfelice,A., Benfante,R., Chelly,J., Billuart,P., Sala,C., *et al.* (2011) A circadian clock in hippocampus is regulated by interaction between oligophrenin-1 and Rev-erbalpha. *Nature Publishing Group*, **14**, 1293–1301.

18. Khelfaoui,M., Gambino,F., Houbaert,X., Ragazzon,B., Muller,C., Carta,M., Lanore,F., Srikumar,B.N., Gastrein,P., Lepleux,M., *et al.* (2013) Lack of the presynaptic RhoGAP protein oligophrenin1 leads to cognitive disabilities through dysregulation of the cAMP/PKA signalling pathway. *Philosophical Transactions of the Royal Society B: Biological Sciences*, **369**, 20130160–20130160.

19. Olson,M.F. (2008) Applications for ROCK kinase inhibition. *Curr. Opin. Cell Biol.*, **20**, 242–248.

20. Hou,Y., Zhou,L., Yang,Q.D., Du,X.P., Li,M., Yuan,M. and Zhou,Z.W. (2012) Changes in hippocampal synapses and learning-memory abilities in a streptozotocin-treated rat model and intervention by using fasudil hydrochloride. *NSC*, **200**, 120–129.

21. Amano,M., Ito,M., Kimura,K., Fukata,Y., Chihara,K., Nakano,T., Matsuura,Y. and Kaibuchi,K. (1996) Phosphorylation and activation of myosin by Rho-associated kinase (Rho-kinase). *Journal of Biological Chemistry*, **271**, 20246–20249.

22. Powell,A.D., Saintot,P.-P., Gill,K.K., Bharathan,A., Buck,S.C., Morris,G., Jiruska,P. and Jefferys,J.G.R. (2014) Reduced Gamma Oscillations in a Mouse Model of Intellectual Disability: A Role for Impaired Repetitive Neurotransmission? *PLoS ONE*, **9**, e95871–10.

23. Chapleau,C.A., Boggio,E.M., Calfa,G., Percy,A.K., Giustetto,M. and Pozzo-Miller,L. (2012) Hippocampal CA1 Pyramidal Neurons of Mecp2Mutant Mice Show a Dendritic Spine Phenotype Only in the Presymptomatic Stage. *Neural Plasticity*, **2012**, 1–9.

24. Durand,C.M., Perroy,J., Loll,F., Perrais,D., Fagni,L., Bourgeron,T., Montcouquiol,M. and Sans,N. (2012) SHANK3 mutations identified in autism lead to modification of dendritic spine morphology via an actin-dependent mechanism. *Molecular Psychiatry*, **17**, 71–84.

25. He,C.X. and Portera-Cailliau,C. (2013) The trouble with spines in fragile X syndrome: density, maturity and plasticity. *Neuroscience*, **251**, 120–128.

26. Nusser,N., Gosmanova,E., Makarova,N., Fujiwara,Y., Yang,L., Guo,F., Luo,Y., Zheng,Y. and Tigyi,G. (2006) Serine phosphorylation differentially affects RhoA binding to effectors: Implications to NGF-induced neurite outgrowth. *Cellular Signalling*, **18**, 704–714.

27. Newell-Litwa,K.A., Badoual,M., Asmussen,H., Patel,H., Whitmore,L. and Horwitz,A.R. (2015) ROCK1 and 2 differentially regulate actomyosin organization to drive cell and

Downloaded from http://hmg.oxfordjournals.org/ by guest on May 5, 2016

synaptic polarity. *The Journal of Cell Biology*, **210**, 225–242.

28. Davies,S.P., Reddy,H., Caivano,M. and Cohen,P. (2000) Specificity and mechanism of action of some commonly used protein kinase inhibitors. *Biochem. J.*, **351**, 95–105.

29. Repetto,D., Camera,P., Melani,R., Morello,N., Russo,I., Calcagno,E., Tomasoni,R., Bianchi,F., Berto,G., Giustetto,M., *et al.* (2014) p140Cap regulates memory and synaptic plasticity through Src-mediated and citron-N-mediated actin reorganization. *The Journal of neuroscience : the official journal of the Society for Neuroscience*, **34**, 1542–1553.

30. Sel,S., Kaiser,M., Nass,N., Trau,S., Roepke,A., Storsberg,J., Hampel,U., Paulsen,F. and Kalinski,T. (2012) Oligophrenin-1 (Ophn1) is expressed in mouse retinal vessels. *Gene Expression Patterns*, **12**, 63–67.

31. Rolli-Derkinderen,M., Toumaniantz,G., Pacaud,P. and Loirand,G. (2010) RhoA Phosphorylation Induces Rac1 Release from Guanine Dissociation Inhibitor and Stimulation of Vascular Smooth Muscle Cell Migration. *Molecular and Cellular Biology*, **30**, 4786–4796.

32. Aquilina,K., Hobbs,C., Cherian,S., Tucker,A., Porter,H., Whitelaw,A. and Thoresen,M. (2007) A neonatal piglet model of intraventricular hemorrhage and posthemorrhagic ventricular dilation. *J. Neurosurg.*, **107**, 126–136.

33. van Nieuw Amerongen,G.P., van Delft,S., Vermeer,M.A., Collard,J.G. and van Hinsbergh,V.W. (2000) Activation of RhoA by thrombin in endothelial hyperpermeability: role of Rho kinase and protein tyrosine kinases. *Circulation Research*, **87**, 335–340.

34. Naert,A., Gantois,I., Laeremans,A., Vreysen,S., Van den Bergh,G., Arckens,L., Callaerts-Vegh,Z. and D'Hooge,R. (2013) Behavioural alterations relevant to developmental brain disorders in mice with neonatally induced ventral hippocampal lesions. *Brain Res. Bull.*, **94**, 71–81.

35. Maksimovic,M., Aitta-aho,T. and Korpi,E.R. (2014) Reversal of novelty-induced hippocampal c-Fos expression in GluA1 subunit-deficient mice by chronic treatment targeting glutamatergic transmission. *European Journal of Pharmacology*, **745**, 36–45.

36. Walsh,J., Desbonnet,L., Clarke,N., Waddington,J.L. and O'Tuathaigh,C.M.P. (2012) Disruption of exploratory and habituation behavior in mice with mutation of DISC1: an ethologically based analysis. *J. Neurosci. Res.*, **90**, 1445–1453.

37. Butruille,L., Mayeur,S., Duparc,T., Knauf,C., Moitrot,E., Fajardy,I., Valet,P., Storme,L., Deruelle,P. and Lesage,J. (2012) Prenatal fasudil exposure alleviates fetal growth but programs hyperphagia and overweight in the adult male rat. *European Journal of Pharmacology*, **689**, 278–284.

38. Castrén,E. and Rantamäki,T. (2010) The role of BDNF and its receptors in depression and antidepressant drug action: Reactivation of developmental plasticity. *Devel Neurobio*, **70**, 289–297.

39. Ehninger,D., Li,W., Fox,K., Stryker,M.P. and Silva,A.J. (2008) Reversing Neurodevelopmental Disorders in Adults. *NEURON*, **60**, 950–960.

40. Hatcher,J.P., Jones,D.N., Rogers,D.C., Hatcher,P.D., Reavill,C., Hagan,J.J. and Hunter,A.J. (2001) Development of SHIRPA to characterise the phenotype of gene-targeted mice. *Behavioural Brain Research*, **125**, 43–47.

Downloaded from http://hmg.oxfordjournals.org/ by guest on May 5, 2016

41. Meziane,H., Schaller,F., Bauer,S., Villard,C., Matarazzo,V., Riet,F., Guillon,G., Lafitte,D., Desarmenien,M.G., Tauber,M., *et al.* (2015) An Early Postnatal Oxytocin Treatment Prevents Social and Learning Deficits in Adult Mice Deficient for Magel2, a Gene Involved in Prader-Willi Syndrome and Autism. *Biological Psychiatry*, **78**, 85–94.

Figure Legends:

Figure 1: RHOA/ROCK signalling pathway and therapeutic schemas.

A. RHOA/ROCK signalling pathway and its inhibition by OPHN1 and by Fasudil (HA1077). RHO: RAS homolog GTPase, ROCK: RHO kinase, MYPT1: Myosin phosphatase target subunit 1, MLC: myosin light chain.

B. First therapeutic scheme: 17 weeks-old (w) males were treated for 12 weeks with a daily dose of 3mg of Fasudil by oral administration. One month after the initial start animals were tested for their behaviour in motor and cognitive tasks that last for 8 weeks before analyses of brain anatomy using Magnetic Resonance Imagery (MRI).

C. Second therapeutic scheme: 8 weeks-old (w) males were treated for 12 weeks with a daily dose of 3mg of Fasudil by oral administration. At the end of the protocol, animals were perfused with fixative for dendritic spines analyses.

Figure 2: Fasudil rescues hyperactivity in *Ophn1*$^{-/y}$ mice.

A. Mean time of latency before falling from the axis in the rotarod test. (n=10-11 mice per group).

B. and C. Mean rearing activity during the 5 first minutes after the introduction of the animals to the elevated-plus maze (B.) or the open field in the object recognition test (Habituation phase) (C.), (n=10-11 mice per group).

D. Mean activity of locomotion in the open field during the first five minutes (n=10-11 mice per group).

Figure 3: Recognition but not working and spatial memories are improved upon Fasudil treatment:

A. Recognition index (%) as measured during the retention phase in the object recognition task.

B. Working memory measured by the spontaneous alternation rate (%) in the Y maze.

C. and D. Spatial reference learning and memory measured by the distance to reach the hidden platform during 5 days of training (C.) and by the number of platform crosses (D.)

Statistical comparisons *: *Ophn1*$^{-/y}$ vs *Ophn1*$^{+/y}$. $: Statically different from the chance (50, line in hyphen).

Figure 4: Fasudil rescues brain ventricular dilatation in *Ophn1*$^{-/y}$ mice

Downloaded from http://hmg.oxfordjournals.org/ by guest on May 5, 2016

A. Delineation of the brain ventricles on MRI slice (filled in red)

B. Mean size of the ventricular normalized to untreated *Ophn1*$^{+/y}$. Statistical comparisons *: *Ophn1*$^{-/y}$ vs *Ophn1*$^{+/y}$, (n=4-6 mice per group).

C. Delineation of the whole brain on MRI slice (surrounded in red)

D. Mean volume of whole brain (in mm^3), (n=4-6 mice per group)

Figure 5: Fasudil treatment differentially affects dentritic spine density and morphology according to genotype.

A. Representative confocal micrograph showing DiOlistic fluorescent labeling of dendritic spines protruding from apical dendrites (100-200 µm from the soma) of CA1 pyramidal neurons in *Ophn1*$^{-/y}$ and *Ophn1*$^{+/y}$ mice treated with Fasudil or vehicle. Scale bar 5 µm.

(B, C, D) Spine density. Quantitative analysis of the density of filopodia- (B), thin-(C) and mushroom-shaped (D) spines in control and Fasudil-treated mice of both genotypes.

(E, F) Spine Morphology. Quantitative analysis of the mean head diameter of thin spines (E) and mean neck length of mushroom-shaped spines (F) in CA1 pyramidal neurons in control and Fasudil-treated animals of both genotypes.

Statistical comparisons: Bonferroni post-tests. *: $p < 0.05$, *Ophn1*$^{-/y}$ vs *Ophn1*$^{+/y}$ and #: $p < 0.05$, untreated vs treated.

Supplemental data1:

Hyperactivity recorded during during the first ten minutes of the acquisition trial in the object recognition task. Left: mean distance in meters (m); Right: number of rears.

Supplemental data2:

A. Post-natal compensation of dendritic spine deficit in *Ophn1*$^{-/y}$ mice; differences between genotype were extrapolated from data in (9, 10)

B. Developmental model of dendritic spine according to genotype. The first months after birth are characterized by the elimination of an excessive number of synapses and by intense remodeling of dendritic spines. Loss of *Ophn1* would accelerate this maturation by increasing RHO activity and retraction of spines compared to “normal” RAC activation. Meanwhile the increase of PKA activity secondary to the inactivation of *Ophn1* will inhibit RHOA/ROCK activation back to controls (5 months). In the presence of Fasudil the balance between RHO and RAC would be differentially affected according to genotype due to Fasudil inhibition of both PKA and ROCK.

C. Model negative regulation of RHO GTPase signaling by PKA. RHOA phosphorylation by PKA inhibits its binding to ROCK but not to CITRON. Fasudil not only inhibits ROCK but also PKA. In the presence of *OPHN1*, both RHOA/ROCK and RHOA/CITRON pathways are inhibited by Fasudil, resulting in the RAC hyperactivation and spine growth. In the absence of *OPHN1*, treatment by Fasudil inhibits both PKA and ROCK but RHOA/CITRON, which is still activated leading to spine retraction.

Downloaded from http://hmg.oxfordjournals.org/ by guest on May 5, 2016

Abbreviations:

Intellectual Disability (ID), Intelligence Quotient (IQ) , Autism Spectrum Disorder (ASD), Central Nervous System (CNS), α-amino-3-hydroxy-5-methyl-4-isoxazolepropionic acid receptor (AMPAR), Post-Synaptic Density (PSD), type1-metabolotropic receptors (mGluR1), Long Term Depression (LTD), myosin phosphatase target subunit-1 (MYPT1), the Myosin light chain (MLC).

Downloaded from http://hmg.oxfordjournals.org/ by guest on May 5, 2016

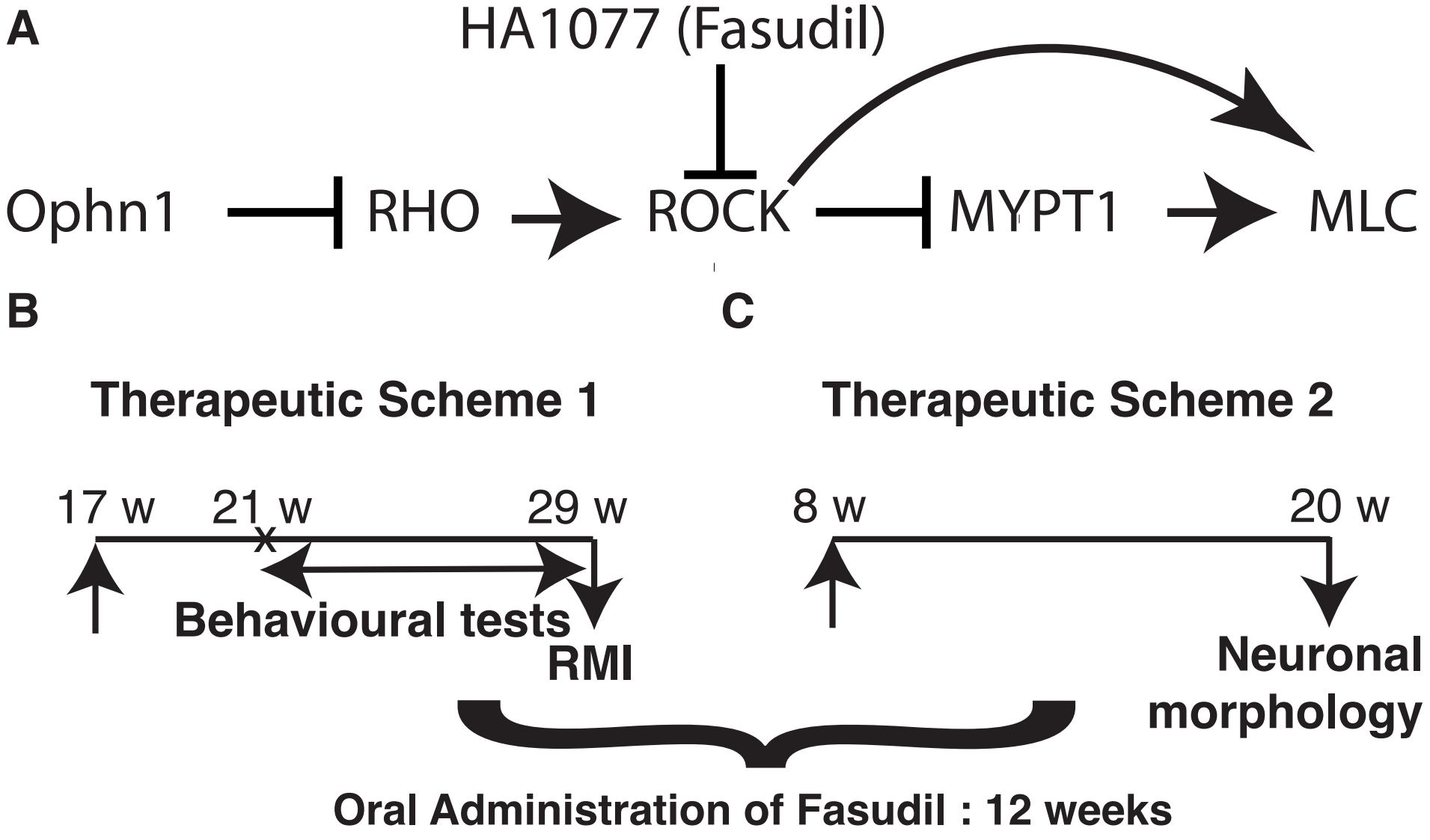
A
HA1077 (Fasudil)
Ophn1
RHO
ROCK
MYPT1
MLC
B
C
Therapeutic Scheme 1
Therapeutic Scheme 2
17 w
21 w
29 w
8 w
20 w
Behavioural tests
RMI
Neuronal morphology
Oral Administration of Fasudil : 12 weeks

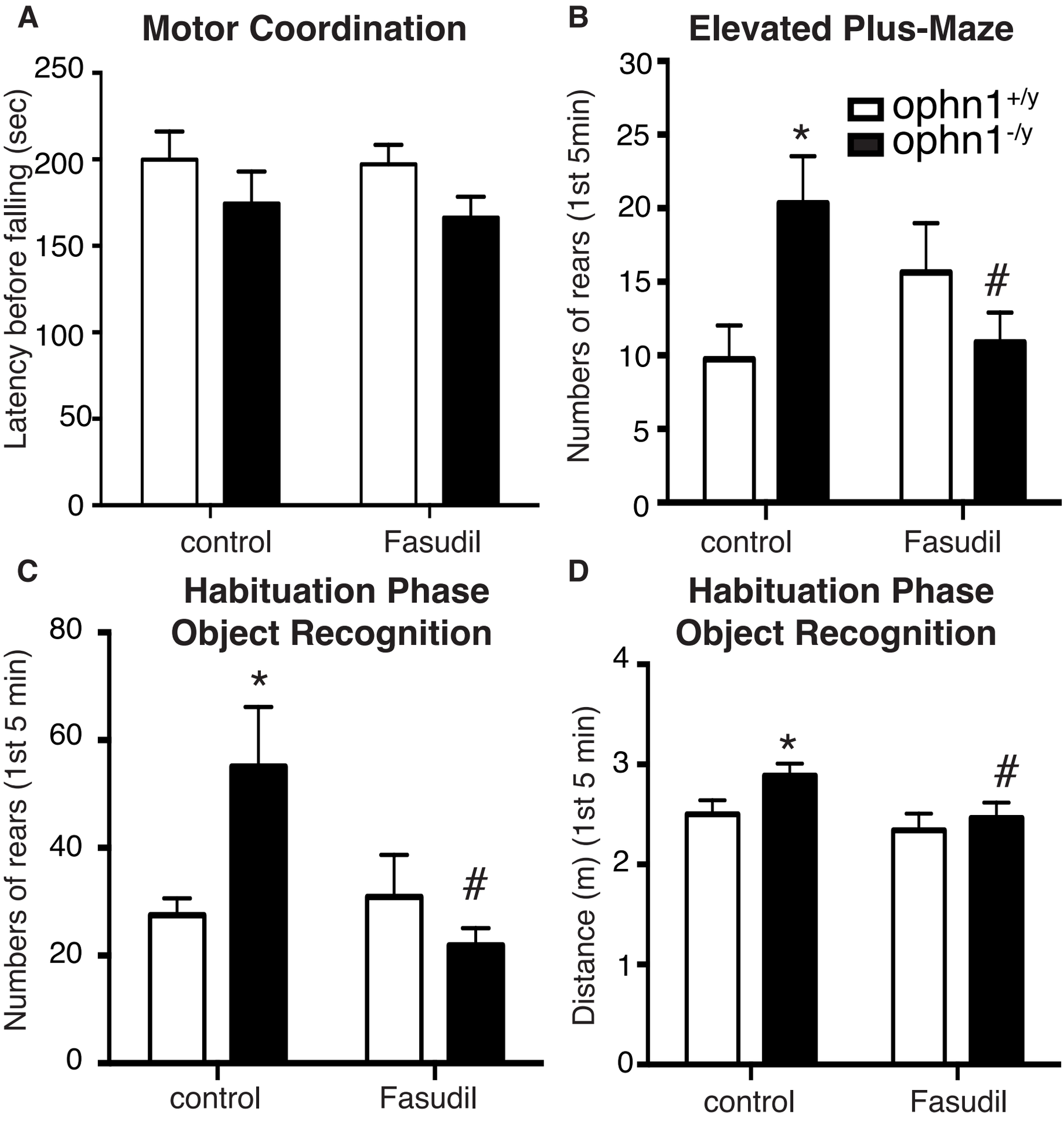
A
Motor Coordination
Latency before falling (sec)
250
200
150
100
50
0
control
Fasudil
B
Elevated Plus-Maze
Numbers of rears (1st 5min)
30
25
20
15
10
5
0
ophn1+/y
ophn1-/y
*
#
control
Fasudil
C
Habituation Phase
Object Recognition
Numbers of rears (1st 5 min)
80
60
40
20
0
*
#
control
Fasudil
D
Habituation Phase
Object Recognition
Distance (m) (1st 5 min)
4
3
2
1
0
*
#
control
Fasudil

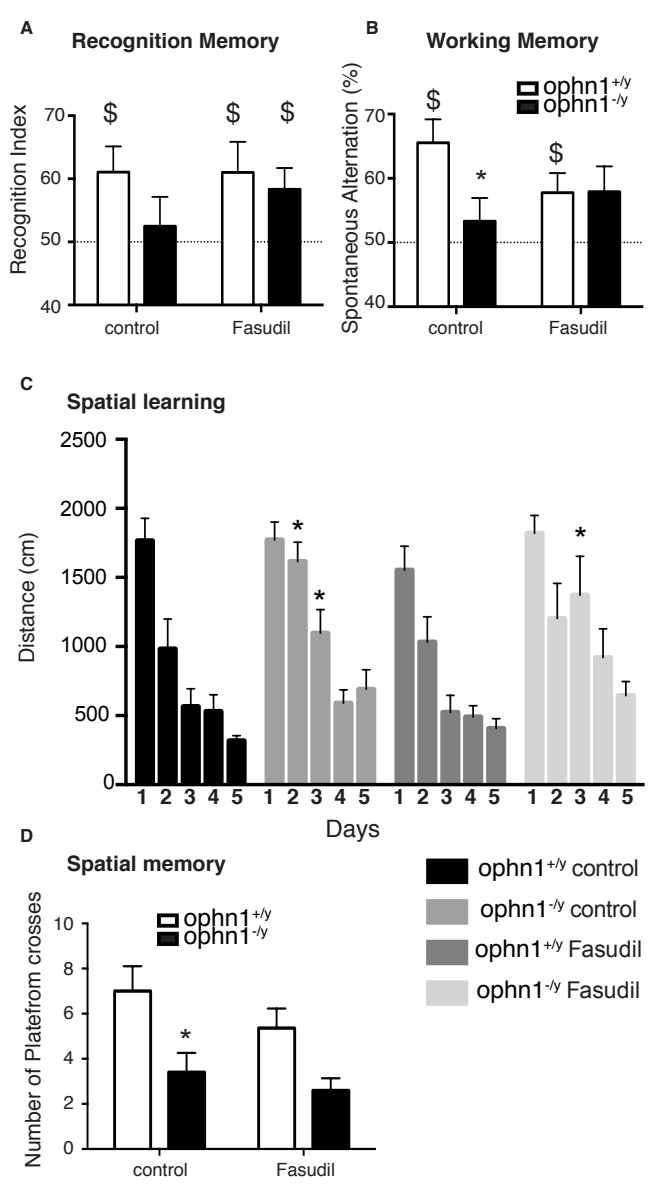
A
Recognition Memory
Recognition Index
70
60
50
40
$
$
$
control
Fasudil
B
Working Memory
Spontaneous Alternation (%)
ophn1+/y
ophn1-/y
70
60
50
40
$
*
$
control
Fasudil
C
Spatial learning
Distance (cm)
2500
2000
1500
1000
500
0
1 2 3 4 5 1 2 3 4 5 1 2 3 4 5 1 2 3 4 5
Days
D
Spatial memory
Number of Platefrom crosses
ophn1+/y
ophn1-/y
10
8
6
4
2
0
*
control
Fasudil
ophn1+/y control
ophn1-/y control
ophn1+/y Fasudil
ophn1-/y Fasudil

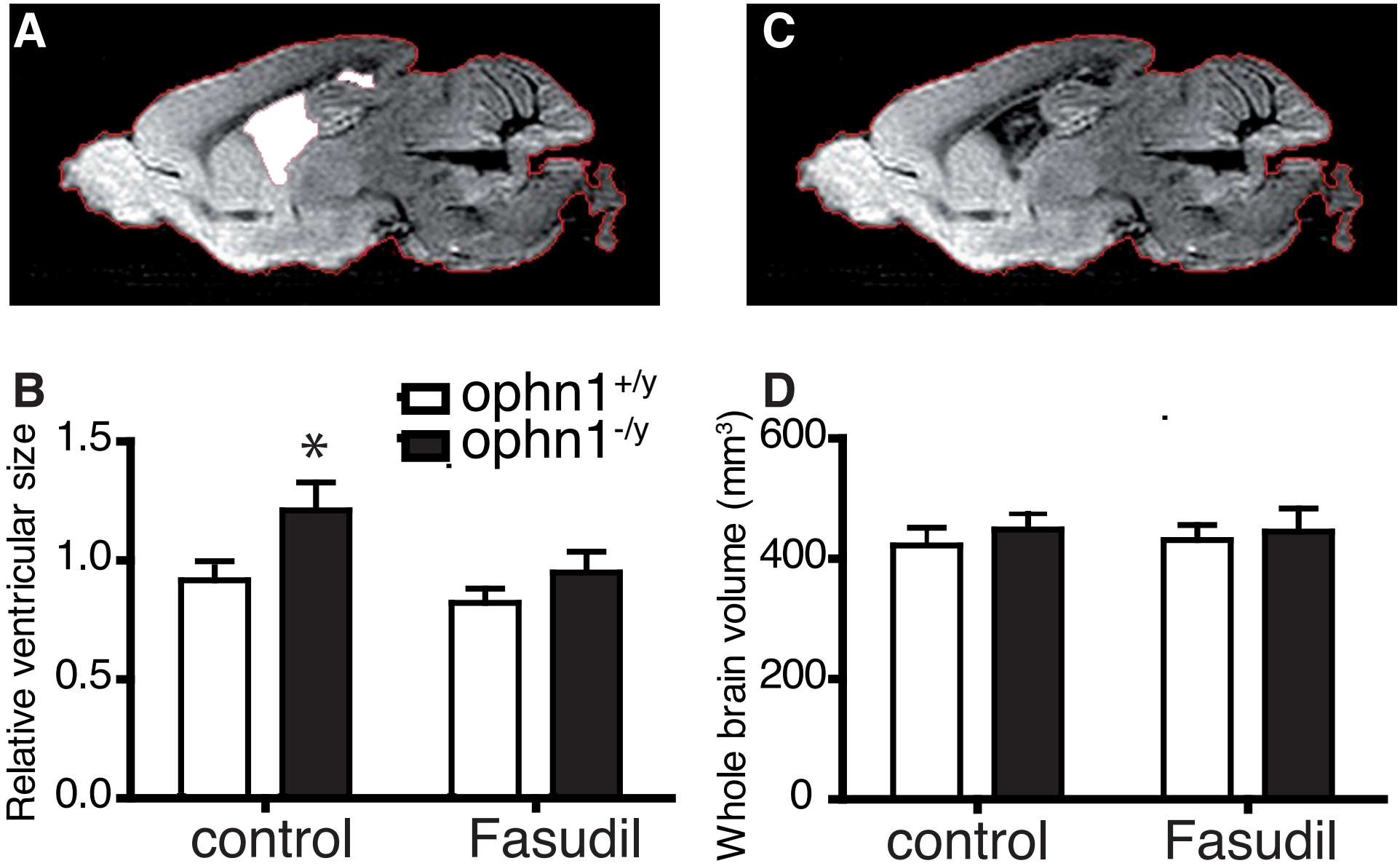
A
C
B
ophn1+/y
ophn1-/y
Relative ventricular size
1.5
1.0
0.5
0.0
*
control
Fasudil
D
Whole brain volume (mm3)
600
400
200
0
control
Fasudil

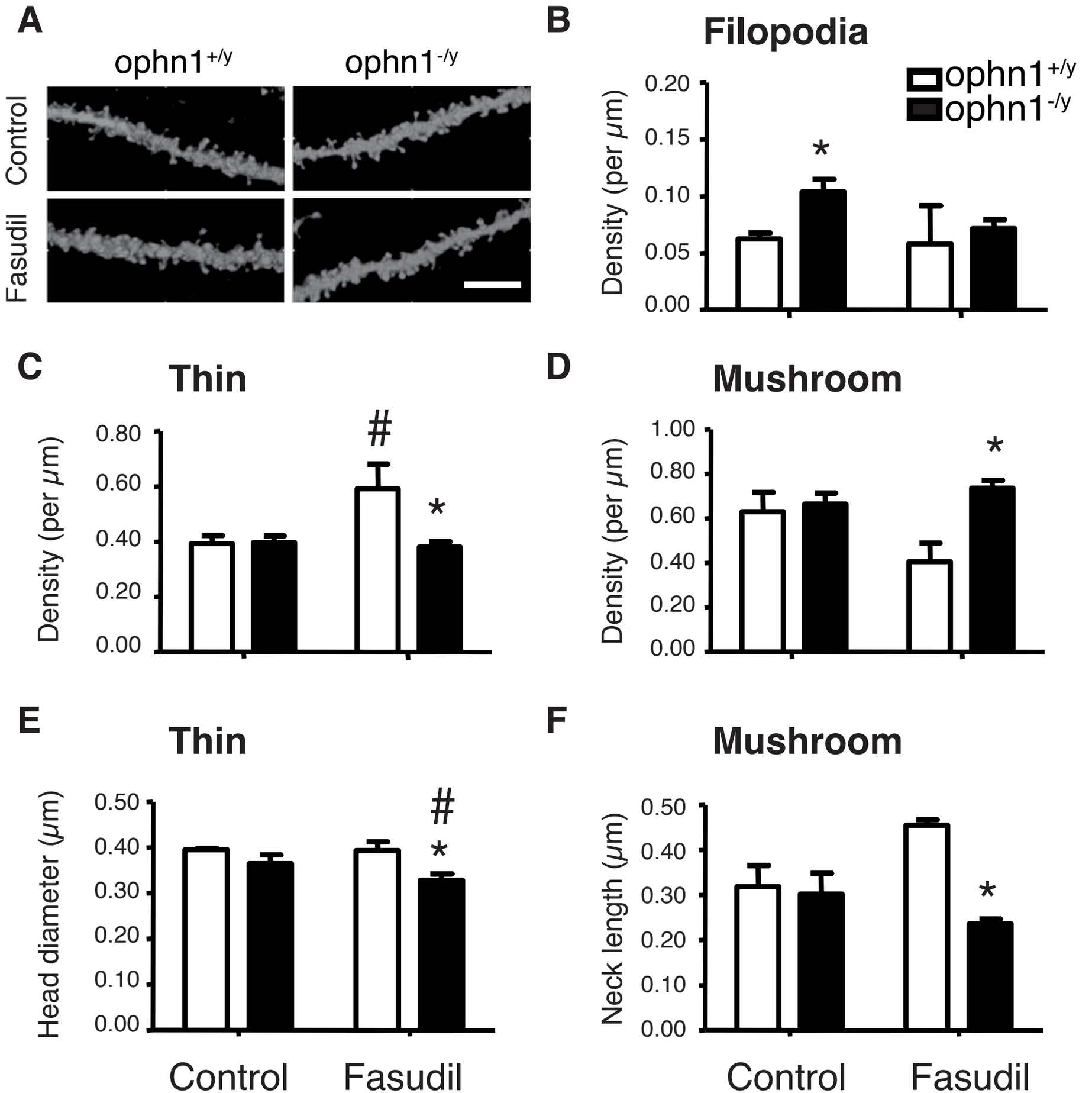
A
ophn1+/y
ophn1-/y
Control
Fasudil
B
Filopodia
ophn1+/y
ophn1-/y
Density (per μm)
0.20
0.15
0.10
0.05
0.00
*
C
Thin
Density (per μm)
0.80
0.60
0.40
0.20
0.00
#
*
D
Mushroom
Density (per μm)
1.00
0.80
0.60
0.40
0.20
0.00
*
E
Thin
Head diameter (μm)
0.50
0.40
0.30
0.20
0.10
0.00
#
*
Control
Fasudil
F
Mushroom
Neck length (μm)
0.50
0.40
0.30
0.20
0.10
0.00
*
Control
Fasudil